Studies of Reactions of Atoms in a Discharge Flow Stirred Reactor
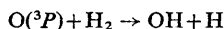
Part 2.—O + H$_2$ + CO System

By Ian M. Campbell * and Brian J. Handy †

School of Chemistry, The University, Leeds LS2 9JT

A discharge–flow stirred reaction system has been used to measure the rate constant for the reaction

$$O(^3P) + H_2 \rightarrow OH + H$$

over the temperature range 315-490 K. Below 350 K, carbon monoxide ($\leqslant 5\%$) was added to generate the bluish O + CO chemiluminescence, the intensity of which served to measure oxygen atom decay rates. An expression $k_1 = (3.1 \pm 0.5) \times 10^{10} \exp(-4950 \pm 300 \text{ K}/T) \text{ dm}^3 \text{ mol}^{-1} \text{ s}^{-1}$ summarised the measurements above 350 K, but sharp positive deviation was found in the Arrhenius plot of k_1 below this temperature, for which quantum mechanical tunnelling in the transition state provides a likely interpretation.

At 425 K in O/H$_2$/N$_2$ or Ar systems with CO mole fractions up to 60%, HCO radicals are synthesised by the combination reaction

$$H + CO + M = HCO + M \tag{19}$$

and destroyed by the reactions

$$H + HCO \rightarrow H_2 + CO \tag{20}$$

$$O + HCO \rightarrow CO + OH \tag{21a}$$

$$O + HCO \rightarrow CO_2 + H. \tag{21b}$$

In systems where large mole fractions of CO were present, the [H]/[O] ratios were established from the linear increase in the oxygen atom decay rate from entry to exit with increasing additions of nitric oxide, using the O + CO chemiluminescence as indicator. In 27 experiments in N$_2$ carriers and 36 experiments in Ar carriers with $90 < \text{[CO]/[O]} < 950$ and $0.2 \leqslant \text{[H]/[O]} \leqslant 3$, the measured oxygen atom decay parameters were analysed iteratively by computer. Combination of these two types of experimental results yielded $k_{19}(\text{M} = \text{N}_2) = (1.44 \pm 0.12) \times 10^8 \text{ dm}^6 \text{ mol}^{-2} \text{ s}^{-1}$ and $k_{19}(\text{M} = \text{Ar}) = (0.97 \pm 0.09) \times 10^8 \text{ dm}^6 \text{ mol}^{-2} \text{ s}^{-1}$ for 425 K, the latter in agreement with temperature extrapolated literature values. A well-defined ratio $A = k_{20}/k_{21} = 2.1 \pm 0.3$ was also obtained, together with an estimate of $B = k_{21a}/k_{21} = 0.4 \pm 0.2$. A simplified collisional model is used to interpret the values of A and B.


In Part 1,[1] the operating principles of a stirred-flow reactor were discussed and a study was made of the kinetics of reactions of HNO, synthesised *in situ* by combination of H atoms with nitric oxide. It was shown that the rate of decay of oxygen atoms reflected the formation and removal kinetics of HNO.

In this paper, the $O(^3P) + H_2 + CO$ system is investigated with a view to measuring the formation and destruction rate parameters for HCO radicals synthesised *in situ* through the three body combination of H atoms and carbon monoxide. This is a novel approach since previous studies of the rates of reaction of HCO radicals with

† Present address: Department of Physical Chemistry, University of Cambridge, Lensfield Road, Cambridge CB2 1EP.

O and H atoms have been based upon the " stripping down " of larger species (ethylene [2] and formaldehyde [3]) in reaction with O atoms to form HCO. Moreover the reactions are studied in the presence of a uniform [H]/[O] ratio in our stirred flow reactor, in contrast to the changing [H]/[O] ratio as a function of reaction time in the previous studies cited above.

The blue chemiluminescence associated with the reaction

$$O + CO + M \rightarrow CO_2 + M$$
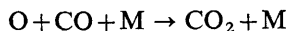
and used to measure oxygen atom decay rates here has allowed the extension of our previous measurements of the rate constant k_1 [ref. (1)] to lower temperatures.

$$O + H_2 \rightarrow OH + H. \tag{1}$$

This is because the overall rate constant of the above O + CO combination reaction is only of the order of $10^6 \, dm^6 \, mol^{-2} \, s^{-1}$ near 300 K [4, 5] as opposed to the order of $10^{10} \, dm^6 \, mol^{-2} \, s^{-1}$ (see Part 1) for k_3 for the combination reaction

$$O + NO + M \rightarrow NO_2 + M$$
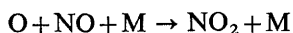
which produced the air afterglow chemiluminescence used in Part 1. The competition of reaction (3) with reaction (1) in the oxygen atom decay rate measured, for sufficient NO addition to give measurable chemiluminescent intensity, made 363 K the lowest temperature at which k_1 could be measured with acceptable precision in Part 1. Here as little as a few percent of CO in the carrier gas gave sufficient chemiluminescent intensity, while even for the highest CO additions the direct combination of O + CO induced no significant term in the oxygen atom decay rate.

It is important to establish reliable values of k_1 in the temperature range below 350 K since there is dispute over the temperature coefficient. Campbell and Thrush [6] measured k_1 at the single temperature of 320 K; their value was substantially larger than that indicated by extrapolation of the Arrhenius expression for k_1 at higher temperatures and they postulated that this indicated quantum mechanical tunnelling in the transition state of reaction (1). However, more recent results obtained by Dubinsky and McKenney,[7] using the air afterglow chemiluminescence in a linear flow system, have been interpreted as indicating a rather lower activation energy over the temperature range 742-347 K than all other studies. Extrapolation of their Arrhenius plot to 320 K agrees with the Campbell and Thrush determination,[6] without the need to invoke quantum mechanical tunnelling.

EXPERIMENTAL

The design and operation of the discharge-flow stirred reactor have been described.[1] General procedures in the present work were similar, so that only significant points of difference will be described in detail.

The central feature is a 0.54 dm^3 Pyrex sphere, internally coated with syrupy phosphoric acid to inhibit wall-recombination of atoms. The entry and exit tubings are non-penetrating and in-line: the entry tubing has inset jets J1 and J2, the latter just upstream of the entry observation station L1, as shown in fig. 1 of Part 1. A modification in the present system is the insertion of a side arm between J1 and J2, through which the calibrated flows of CO were added. The upstream jet, J1, was used to titrate $N(^4S)$ atoms coming from the discharge with nitric oxide, so generating known concentrations of $O(^3P)$ atoms according to the rapid and stoichiometric reaction

$$N(^4S) + NO \rightarrow N_2 + O(^3P).$$
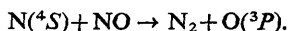
The disappearance of visible emission in the tubing between J1 and the CO addition side arm marked the end point of the titration. The jet J2 was used to add calibrated flows of nitric oxide or molecular oxygen as before. The intensities of the bluish O + CO chemi-

luminescence were measured at the observation points L1 (entry) and L2 (exit) using an RCA 1P28 photomultiplier viewing through an Oriel Optics G-774-3550 filter, transmitting between 290 and 410 nm and thus opaque to the air afterglow ($O+NO$) emission. Since the CO is always present in large excess and the intensity of the blue emission is proportional to [O][CO],[8] the photomultiplier signal, displayed on a Pye Scalamp galvanometer, was proportional to [O]. The intercalibration of the observation ports for $O+CO$ emission was performed in the same manner as described for $O+NO$ emission in Part 1, *viz.* using high flowrates at low pressures when a column of glowing gas passed from entry to exit throat across the sphere. Under these circumstances, the detected change in signal from L1 to L2 could only be due to viscous flow pressure drops in the tubings, which were calculable. The resultant factor was used to correct the relative signals measured when the system was operated in the stirred-flow mode, *i.e.* lower total flowrates ($\leqslant 100\mu$ mol s^{-1}) and higher pressures ($\geqslant 0.3$ kPa).

Carbon monoxide was taken from a cylinder (Air Products) and was purified by passage over quartz chips heated to ~ 1000 K, in order to decompose carbonyls, *etc.* The gas then flowed at pressure just below atmospheric through a spiral trap and a U-trap packed with activated silica gel, both maintained at 195 K with Cardice. The flowrate was regulated using a needle valve and measured using a calibrated capillary flowmeter on the high pressure side. In calibration of this capillary, advantage was taken of the near identical viscosity coefficients of CO and N_2; N_2 was used as the calibrating gas in conjunction with a bubble flowmeter open to the atmosphere.

Calibrated flows of hydrogen were added through the side arms of the sphere. This and the other gases were purified and delivered as described in Part 1.

RESULTS AND DISCUSSION

MEASUREMENT OF k_1

When only small additions of CO ($\leqslant 5\%$) were made, the reactions

$$O+H_2 \rightarrow OH+H \tag{1}$$

$$O+OH \rightarrow O_2+H \tag{2}$$
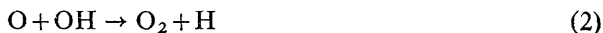
could be made to dominate the rate of O atom decay, with reaction (1) rate determining. The slight competition for OH radicals between reactions (2) and (18) (reaction numbering scheme continuous from Part 1)

$$CO+OH \rightarrow CO_2+H \tag{18}$$

was corrected for using our recent measurement[9] of $k_2/k_{18} = 260 \pm 20$.

Reaction (1) is slow at temperatures below 350 K so that substantial replacement (up to 50%) of the N_2 carrier by H_2 was required to produce easily measurable O atom decays in the reactor. In Part 1 it was demonstrated that stirred flow operation was maintained when up to half the carrier gas was added through the side arms of the sphere. But since H_2 is not present in the entry tubing, the signal measured at L2 has to be increased to take account of the dilution effect on both [O] and [CO] in the exit tubing. At the same time it is likely that H_2 will have an enhancement/quenching effect on the $O+CO$ emission efficiency compared with N_2. This effect was estimated at L1 in the entry tubing under relatively fast flow conditions at room temperature, on the reasonable assumption of temperature invariance up to 350 K. Varying flows of H_2 were added together with a constant small flow of CO through the side arm between J1 and J2 and the total pressure was maintained constant by adjustment of the large tap at the downstream end of the exit tubing. Since O atom decay would be negligible under these conditions between the side arm and L1, the variation of $I/$[O][CO], where I is the measured signal and [O] is established by the titration at J1 reduced in proportion to the dilution by CO and H_2, could only

reflect carrier gas composition effects. A small linear enhancement of $I/[O][CO]$ with increasing mol fraction of H_2 was found, extrapolating to a factor of 1.15 for $M = H_2$ compared with $M = N_2$. Separate experiments showed that there was no significant variation in $I/[O][CO]$ as a function of increasing CO mol fraction in N_2 up to 0.6. The effect was taken into account by making a small reduction of the signal at L2 in proportion to the mole fraction of H_2.

In the presence of the substantial mole fractions of H_2 used in the low temperature region, the reaction

$$OH + H_2 \rightarrow H_2O + H \tag{12}$$

achieved a minor rate ($\leqslant 5\%$) relative to that of reaction (2). The rate constant is well-established and was derived from the expression evaluated by Baulch et al.[10] A further small correction to the decay originated from the O_2 formed in the system and the catalytic cycle

$$H + O_2 + M \rightarrow HO_2 + M \tag{9}$$

$$H + HO_2 \rightarrow 2OH \tag{10}$$

$$O + HO_2 \rightarrow OH + O_2. \tag{11}$$

This was estimated directly in each run by observing the linear increase in $-\Delta[O]/[O]$ [$= (I_1 - I_2)/I_2$] with [O_2], when known flowrates of O_2 were added at J1, and back-extrapolation to $[O_2] = 0$. Another small correction arose from HCO formation and reaction with O atoms; this was assessed for each run using the rate parameters for HCO reactions given later.

It should be emphasized that the net correction for conversion of the measured $-\Delta[O]/[O]$ into the corrected parameter $-(\Delta[O]/[O])_c$ is quite small ($\leqslant 10\%$). Thus little additional uncertainty is induced by any uncertainties in the correction rate constants applied. Since reaction (1) is rate determining the analytical relationship predicted is

$$-[\Delta[O]/([O]\Delta t)]_c = 2k_1[H_2]$$

where Δt is the residence time in the sphere.

Plots of $-[\Delta[O]/([O]\Delta t)]_c$ versus [H_2] proved to be linear within the random scatter and yielded values of k_1 over the temperature range 425-315 K plotted in Arrhenius form in fig. 1. Also shown in fig. 1 are the values of k_1 derived in Part 1 using the air afterglow chemiluminescence. The two sets of data overlap well and together cover the temperature range 490-315 K. As was pointed out in Part 1, the Arrhenius expression $k_1 = (3.1 \pm 0.5) \times 10^{10} \exp(-4950 \pm 300 \, K/T)$ dm^3 mol^{-1} s^{-1} for the data above 360 K is in good agreement with the results of most other workers. Our results from O + CO systems represents the first major extension below 350 K. The importance of this is apparent from fig. 1 in the positive deviation away from the Arrhenius line, which comes in quite sharply and amounts to approximately a factor of 2 at 315 K. Campbell and Thrush[6] measured k_1 at 320 K by addition of H_2 to N + O systems and their result shown in fig. 1 agrees with our present values within the respective error limits.

The mean results of Dubinsky and McKenney[7] are also shown in fig. 1 and can be seen to be in reasonable agreement with ours. However they interpreted their results in terms of an Arrhenius line of reduced slope (dashed line in fig. 1) compared with all previous workers. Our more extensive data in the low temperature region show that this Arrhenius line does not accord with our values of k_1 between 380 and 330 K, which lie without exception, below the dashed line. Dubinsky and McKenney's mean value of k_1 at 347 K appears to be in better agreement with our neighbouring points than with their Arrhenius line.
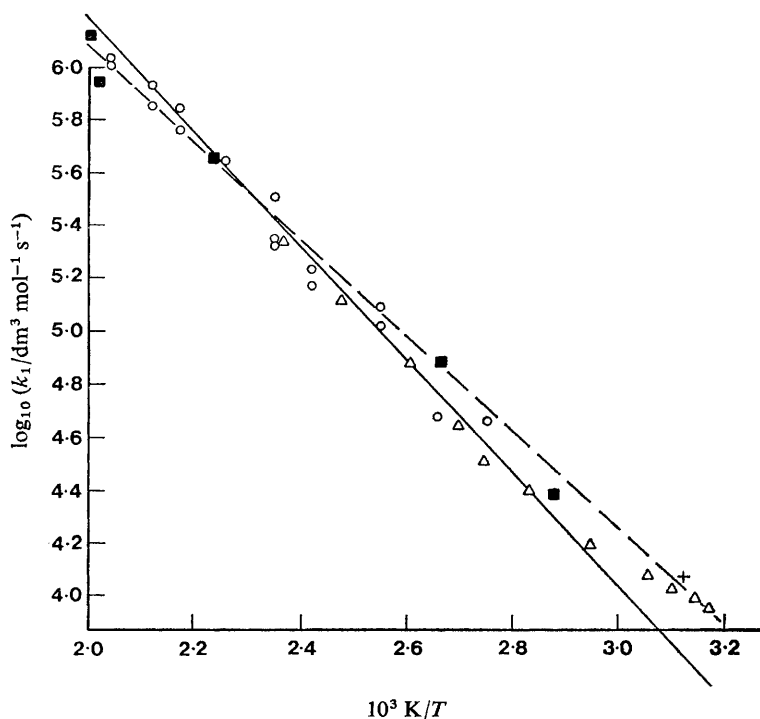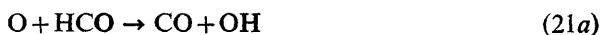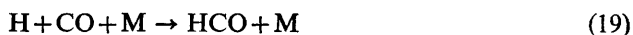
I—11

FIG. 1.—Arrhenius plot of k_1, showing results from present work ($\triangle$), Part 1 ($\bigcirc$), Dubinsky and McKenney[7] ($\blacksquare$) and Campbell and Thrush[6] (+). The full line is the best fit to our data for $350 < T < 490$ K while the dashed line corresponds to the Arrhenius expression given by Dubinsky and McKenney.[7]

Our data for k_1 can be interpreted as the entry of quantum mechanical tunnelling in the transition state as a significant phenomenon below 350 K, when the apparent A factor and activation energy in the Arrhenius expression for k_1 would be expected to decrease with decreasing temperature. This was the interpretation originally advanced by Campbell and Thrush[6] to account for their value at 320 K. Further data below 315 K would be needed before any detailed theoretical interpretation in terms of the configurations and properties of the transition state could be attempted meaningfully. But our data leave little doubt that k_1 does deviate positively below ~ 350 K from the Arrhenius plot for higher temperature data and that the effect comes in quite sharply with decreasing temperature.
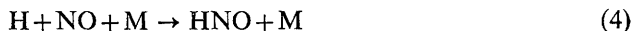
REACTIONS OF HCO RADICALS

When larger additions of CO (up to 60%) were made to $O+H_2$ systems, HCO radicals were synthesized and destroyed at substantial rates in the reaction scheme:

$$H+CO+M \rightarrow HCO+M \tag{19}$$

$$H+HCO \rightarrow H_2+CO \tag{20}$$

$$O+HCO \rightarrow CO+OH \tag{21a}$$

$$O+HCO \rightarrow CO_2+H. \tag{21b}$$

The objectives of our experiments were the measurement of k_{19} and the destruction rate constant ratios $A = k_{20}/k_{21}$ and $B = k_{21a}/k_{21}$. The principle of our method was that, since reaction (21a) produces an OH radical, variation of the [CO]/[O] ratio in the reactor would vary the competition for OH between reactions (2) and (18). Reactions (21a) and (2) remove two O atoms per cycle while reactions (21a) and (18) remove only one O atom per cycle. Since $k_2/k_{18} \simeq 260$,[9] the systems with highest [CO]/[O] ratios render reactions (21a) and (21b) almost equivalent in terms of O atom consumption since $\sim 80\%$ of the OH radicals from reaction (21a) will react in reaction (18). Therefore it was expected that well-defined values of k_{19} and A would be obtained from such experiments but that B would be more difficult to evaluate since systems with low [CO]/[O] ratios produce smaller catalytic rates of O atom removal.

Our preferred working temperature was 425 K, when k_1 has a value which allowed [H]/[O] ratios in the reactor to be adjusted over a wide range (0.2 to 3) when H_2 was only a small fraction ($\leqslant 4\%$) of the total carrier gas but reaction (1) proceeded under pseudo-first order conditions ([H_2] $\gg$ [O]). Conditions could be adjusted so that up to 50% of the total O atom decay rate originated in the cycle of reactions (19)-(21).

Two parameters can be measured for the evaluation of rate constants, the decay rate $-[\Delta[O]/([O]\Delta t)]_c$ and the [H]/[O] ratio. The method of obtaining the latter depends upon the acceleration of the former parameter upon addition of calibrated flowrates of NO at jet J2. The additional reactions with significant rates induced are:

$$O + NO + M \rightarrow NO_2 + M \qquad (3)$$

$$H + NO_2 \rightarrow OH + NO \qquad (13)$$

$$H + NO + M \rightarrow HNO + M \qquad (4)$$

$$O + HNO \rightarrow OH + NO. \qquad (5)$$

Recent absolute measurements of k_{13} [11] indicate a mean value of 1.3×10^{11} dm³ mol⁻¹ s⁻¹ for 425 K, which is some 30 times larger than the rate constant for O atom attack on NO_2 on the basis of the most recent measurements of that.[12] Accordingly reaction (13) can be taken as the overwhelming subsequent step to reaction (3) under our conditions. At the same time, reaction (5) will follow reaction (4) on the basis of our findings in Part 1. The presence of NO then does not alter [H]/[O] since the OH radicals go on to react in either reaction (2) or (18) to regenerate the H atom, while steady state analysis shows

$$\frac{[H]}{[O]} \simeq \frac{2k_1[H_2]\Delta t}{1 + 2k_{19}[CO][M]\Delta t\{A/(A + [O]/[H])\}}. \qquad (i)$$

If we define the parameter $r = k_2[O]/(k_2[O] + k_{18}[CO])$, then the predicted equation for the variation of $-[\Delta[O]/([O]\Delta t)]_c$ with [NO] is

$$\frac{-\{\Delta[O]/([O]\Delta t)\}_c}{1 + r} = \text{constant} + k_3[NO][M] + k_4([H]/[O])[NO][M]. \qquad (ii)$$

The constant will derive from reaction (1) and also the reactions (21) in any one run and is expressed by eqn (iii) below.

Fig. 2 shows the linear enhancements of the decay parameter as a function of added [NO] under various conditions with constant total pressure at 425 K. Plot (a) is for N_2 carrier alone; there is no intercept (showing the absence of wall decay) and the gradient reflects k_3 only. Plot (b) shows the effect of $\sim 3\%$ added H_2; the intercept is equal to $k_1[H_2]$ and the steeper gradient reflects k_4 and [H]/[O] in

REACTIONS OF $O + H_2 + CO$

addition to k_3. Plot (c) represents an attempt to produce the same $[H]/[O]$ ratio [*i.e.* same gradient on the basis of eqn (ii)] in the presence of 25% CO: more H_2 had to be added (as shown by the increased intercept), reflecting the consumption of H atoms through reaction (19) followed by (20). Finally plot (d) shows the effect of addition of the same amount of H_2 as in (c) to the system without CO; the increased gradient reflects the resultant increase in $[H]/[O]$ ratio while the slight decrease in the
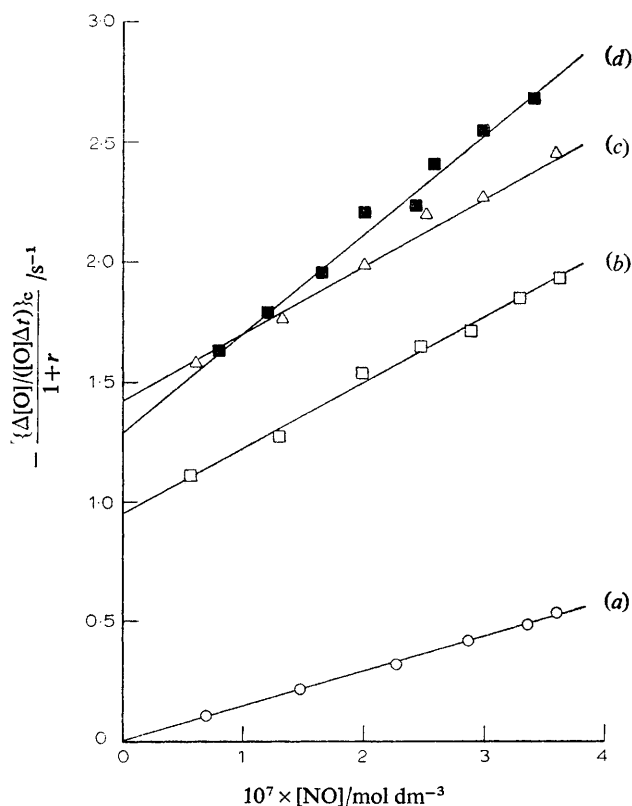

FIG. 2.—Plots of the oxygen atom decay parameter (see text) against NO for $[M] = 1 \times 10^{-4}$ mol dm^{-3} at 425 K. (a) O in N_2 carrier only, (b) O in N_2 carrier with $[H_2] = 3.6 \times 10^{-6}$ mol dm^{-3}, (c) O in N_2 carrier with $[CO] = 2.5 \times 10^{-5}$ mol dm^{-3} and $[H_2] = 5.0 \times 10^{-6}$ mol dm^{-3}, (d) O in N_2 carrier with $[H_2] = 5.1 \times 10^{-6}$ mol dm^{-3}.

intercept between (c) and (d) reflects reactions (19) and (21) in (c). It is then clear that with the knowledge of the values of k_3 and k_4 from Part 1, the gradient of plots such as (c) gives us $[H]/[O]$. At the same time the intercept yields the decay parameter

$$\frac{-\{\Delta[O]/([O]\Delta t)\}_c}{1+r} = k_1[H_2] + k_{19}([H]/[O])[CO][M]Q \qquad \text{(iii)}$$

with $Q = (1 + Br)/\{(1+r)(1 + A[H]/[O])\}$.

An iterative method was employed to extract values of the three unknown parameters k_{19}, A and B.

The first stage of the analysis concerned the extraction of an approximate value of k_{19} from the measurement of $[H]/[O]$ ratios in runs where these were well in

excess of unity. It can be seen that the eqn (i) for [H]/[O] involves only k_{19} and A as unknowns. The previous measurements of A (see table 2) suggest that its value is considerably greater than 1, so that we have made the good first approximation that $A \approx A + [O]/[H]$ to extract the first estimates of k_{19}, designated $k_{19}(1)$ in table 1. This table shows a selection of our measurements of [H]/[O] ratios over a range of pressures in N_2 and Ar carriers. The final values of k_{19} obtained from each run using the value of $A = 2.1$ to follow are shown. The mean value for M = N_2 was $k_{19} = (1.44 \pm 0.12) \times 10^8$ dm^6 mol^{-2} s^{-1} for 425 K, with standard deviation

TABLE 1.—MEASURED [H]/[O] RATIOS AND VALUES OF k_{19} AT 425 K

$10^4[M]$ /mol dm^{-3}	[CO]/[M]	$10^{-6}A$ /dm^3 mol^{-1} s^{-1}	[H]/[O]	$10^{-8}k_{19}(1)$ /dm^6 mol^{-2} s^{-1}	$10^{-8}k_{19}$
M = N$_2$					
0.985	0.250	2.90	1.45	0.99	1.32
1.05	0.352	2.66	1.33	0.98	1.33
1.21	0.303	3.68	2.05	1.01	1.25
1.22	0.300	3.56	2.04	1.20	1.50
1.23	0.298	3.52	2.02	1.31	1.60
1.24	0.306	3.58	2.12	1.33	1.63
2.13	0.256	9.85	3.12	1.34	1.54
2.46	0.249	14.4	3.56	1.22	1.39
2.89	0.223	16.4	3.42	1.19	1.36
M = Ar					
1.16	0.158	3.42	2.11	0.66	0.81
1.20	0.153	3.58	2.09	0.79	0.96
1.20	0.153	3.55	2.09	0.77	0.95
1.21	0.250	3.72	1.95	0.69	0.86
1.22	0.248	3.68	1.98	0.82	1.01
1.22	0.248	3.65	1.95	0.88	1.06
1.31	0.157	4.46	2.66	0.87	1.02

error limits, with total pressure varied over a factor of ~ 3. In view of the similar natures of N_2 and CO, it could be expected that both would have similar third body efficiencies in reactions (3), (4) and (19); no evidence against these expectations was found in any of the experiments. For M = Ar, $k_{19} = (9.7 \pm 0.9) \times 10^7$ dm^6 mol^{-2} s^{-1} for 425 K. The relative third body efficiencies are therefore N_2 : Ar : : (1.48 $\pm$ 0.26) : 1.

Hikida, Eyre and Dorfman [13] have measured $k_{19} = (2.6 \pm 0.4) \times 10^7$ dm^6 mol^{-2} s^{-1} for M = Ar at 298 K in a direct method based upon pulse radiolysis of $H_2 + CO + Ar$ mixtures using Lyman α absorptiometry to monitor the H atom decay rate. Wang, Eyre and Dorfman [14] extended this study over the range 298-373 K for M = H_2, finding a small positive temperature coefficient equivalent to an activation energy of 8.3 ± 1.6 kJ mol^{-1}. On the assumption that the same temperature coefficient applies to k_{19} for M = Ar, this predicts a value of $(7 \pm 3) \times 10^7$ dm^6 mol^{-2} s^{-1} for 425 K, in good agreement with our value above considering the very different techniques.

The approximate $k_{19}(1)$ was applied to the analysis of the O atom decay parameter $-\{\Delta[O]/[O]\Delta t)\}_c$ in the first iteration. [H]/[O] ratios ranged from 0.2 to 3 (established by NO addition) and [CO]/[O] ratios were varied from 90 to 950, again at 425 K. In 27 experiments in N_2 carrier and 36 in Ar carrier, $k_{19}(1)$ was used to extract approximate values of A and B. The former was then reapplied to the data of table 1 and eqn (i) to obtain an improved estimate of k_{19}, which was then used in turn to

improve the estimates of A and B. A computer program was used for the successive iterations which finally produced values of k_{19}, A and B minimizing the sum of the squares of deviations between the observed and predicted values of $-\{\Delta[O]/([O]\Delta t)\}_c$ and $[H]/[O]$. In the N_2 carrier, A was found to be 2.08 ± 0.16, in excellent agreement with $A = 2.03\pm0.14$ in Ar carrier. The value of A proved to be relatively insensitive to variations of k_{19} within the error limits quoted above and $A = 2.1\pm0.3$ encompassed the overall variation. The values of B were much more sensitive to the value of k_{19} applied; even variation of k_{19} within the standard deviation range caused B to change by over a factor of 2 in N_2 carriers with a mean value of 0.25 compared to 0.49 in Ar carriers. Accordingly we recognize the limitations of our method in this respect in merely quoting $B = 0.4\pm0.2$, which covered the bulk of the results.

Table 2 compares these results with existing literature values. It is clear that our

TABLE 2.—COMPARISON OF MEASUREMENTS OF PARAMETERS A AND B

T/K	$A(k_{20}/k_{21})$	$B(k_{21a}/k_{21})$	ref.
300	3 ±2	0.8 ±0.1	2
300	4 ±1	0.54±0.04	3
300	—	0.58±0.06	15
425	2.1±0.3	0.4 ±0.2	this work

value of A is more precisely defined and is lower than the other mean values. However, in the other studies the H atoms and HCO radicals were formed as products of reactions between O atoms and ethylene [2] or formaldehyde [3] in flowtubes; thus the H atom concentrations were usually less than those of O atoms and both varied with reaction time, contrasting sharply with our conditions. Our results and their error limits indicate that our method is considerably better for the evaluation of A but we should have to concede that our method is less good for B.

There is one absolute measurement [16] of $k_{21} = (1.3\pm0.2)\times10^{11}$ dm^3 mol^{-1} s^{-1} at 297 K available in the literature; this was obtained by observation of the initial rate of growth of [HCO] in $O(^3P)+C_2H_4$ systems using a photoionization mass spectrometer coupled to a discharge flow tube. This is so close to the collision frequency of O+HCO that it could be expected to have no temperature coefficient; thus the measurements of A and B should be applicable for all normal temperatures. If both H and O atoms had reacted at every collision with HCO, then A should have been ~ 3.3 on the basis of the reduced masses of the collision complexes, approximately double our value. But in the simplest terms, the O atom can be considered to react whichever end of HCO it approaches in reactions (21a) or (21b); the value of B of ~ 0.5 evident in table 2 supports this view. However, the H atom can only react if it approaches the hydrogen end of HCO; interaction with carbonyl end might only result in H atom exchange. Thus our value of A may reflect the availability of only the single channel (20) for the H atom reaction as opposed to the two channels available for O atom reaction expressed by reactions (21a) and (21b).

[1] I. M. Campbell and B. J. Handy, *J.C.S. Faraday I*, 1975, **71**, 2097.
[2] H. Niki, E. E. Daby and B. Weinstock, *Proc. 12th Symp. Combustion* (Combustion Institute, Pittsburgh, 1969), p. 277.
[3] G. P. R. Mack and B. A. Thrush, *J.C.S. Faraday I*, 1973, **69**, 208.
[4] T. G. Slanger, B. J. Wood and G. Black, *J. Chem. Phys.*, 1972, **57**, 233.
[5] F. Stuhl and H. Niki, *J. Chem. Phys.*, 1971, **55**, 3943.

[6] I. M. Campbell and B. A. Thrush, *Trans. Faraday Soc.*, 1968, **64,** 1265.
[7] R. N. Dubinsky and D. J. McKenney, *Canad. J. Chem.*, 1975, **53,** 3531.
[8] M. A. A. Clyne and B. A. Thrush, *Proc. Roy. Soc. A*, 1962, **269,** 404.
[9] I. M. Campbell and B. J. Handy, *Chem. Phys. Letters*, 1977, **47,** 475.
[10] D. L. Baulch, D. D. Drysdale, D. G. Horne and A. C. Lloyd, *Evaluated Kinetic Data for High Temperature Reactions* (Butterworths, London, 1972), vol. 1, p. 77.
[11] H. Gg. Wagner, U. Welzbacher and R. Zellner, *Ber. Bunsenges. phys. Chem.*, 1976, **80,** 1023.
[12] P. P. Bemand, M. A. A. Clyne and R. T. Watson, *J.C.S. Faraday II*, 1974, **70,** 564.
[13] T. Hikida, J. A. Eyre and L. M. Dorfman, *J. Chem. Phys.*, 1971, **54,** 3422.
[14] H. Y. Wang, J. A. Eyre and L. M. Dorfman, *J. Chem. Phys.*, 1973, **59,** 5199.
[15] A. A. Westenberg and N. de Haas, *J. Phys. Chem.*, 1972, **76,** 2215.
[16] N. Washida, R. I. Martinez and K. D. Bayes, *Z. Naturforsch.*, 1974, **29a,** 251.

(PAPER 7/659)